

# A Computational Fluid Dynamics Study of Modeling and Hydrodynamic Characteristics of a Bionic Undulating Fin

Thanh-Long Le<sup>1,2,\*</sup>, Phan Trung Dat<sup>1,2</sup>

<sup>1</sup>Faculty of Mechanical Engineering, Ho Chi Minh City University of Technology (HCMUT), 268 Ly Thuong Kiet Street, District 10, Ho Chi Minh City, Vietnam

<sup>2</sup>Vietnam National University Ho Chi Minh City, Linh Trung Ward, Thu Duc City, Ho Chi Minh City, Vietnam

\*Corresponding author. E-mail: [ltlong@hcmut.edu.vn](mailto:ltlong@hcmut.edu.vn)

## Abstract

Many factors affect the motion of an undulating fin robot. One of them, the most common is the shape of the fish's fins as well as the swimming speed of the robot. In this paper, a waveform fin is investigated at different profiles and flow velocities to predict the hydrodynamic drag acting on the model. In addition, the surrounding flow characteristics were also explored. The model's curved shape was built using ANSYS Spaceclaim. Then the flow and operation region surrounding the model of a bionic undulating fin were established. Specifically, the  $k - \epsilon$  turbulence model is used in this simulation. The Navier-Stokes equations, the energy and momentum conservation equations, and some appropriate boundary conditions were also numerically calculated by ANSYS Fluent. The flow velocity field obtained in the case of the oscillating fin has demonstrated that this is a form of oscillation that generates an auxiliary thrust, helps the robot move forward. In addition, the resistance is observed to decrease when the number of waves on the profile is reduced from three down to one. In contrast, as the robot moves faster, the drag force tends to increase. The obtained simulation results are similar to Curet's actual experiments, showing the utility of using CFD in the future design of autonomous underwater robots.

**Keywords:** CFD, Hydrodynamic, Drag force, Undulating fin, Numerical method.

## 1 Introduction

In recent years, biomimetic robots have attracted much attention from scientists around the world. There have been many robots and equipment designed inspired by the movement and aerodynamic shape of natural creatures such as birds, sharks, dolphins, etc. Among the many interesting features of animals, the undulating fin of the black ghost knife fish can be mentioned. When oscillating, the fin creates a wave that moves along the body and propels the fish forward. With this feature, it allows this fish to move fast in the narrow environment without causing too much disturbance to the surrounding environment like a propeller or water jet engine.

Several authors have designed and studied the propulsion efficiency, power consumption, and force of the knife fish model to improve the speed of the robot in the water [1-3]. In another study, Curet et al. [4] designed a mechatronics system of the fin to control all parameters such as frequency, amplitude, wavelength, angle attack, or flow velocity systematically. Thus, an ideal working scope of these parameters was explored. Furthermore, drag force measurements were also conducted. Inspired by the wave-like swimming of marine species, Han Zhou et al. [5] simulated those movements to provide the pressure distribution near the fish body surface, thereby predicting the flow velocity as well as disturbance to recognize obstacles, keep speed and reduce energy consumption.

Fluid mechanics and Computational Fluid Dynamics (CFD) are rapidly developing fields and have been received various achievements in theory and experimentation. It is a very useful tool to solve numerical problems related to fluid mechanics and be widely applied in many different industries. Various applications of CFD were presented by Le et al. [6-11] to study the behaviors and characteristics of the fluids. Neveln et al. [12] conducted experiments and numerical simulations to study the flow around the robot's fins and demonstrated that it produces thrust during oscillation. Zhang et al. [13] studied the effect of a wavering plate on the performance of the fin. They used the finite volume method (FVM) to simulate a plate oscillating in front of the model and see if different types of plate's motion affect the productivity of the fin. Their results showed that the fin can boost performance by receiving additional energy from the vortices. On the other hand, Zhang realized that by increasing the frequency of the plate, the produced thrust force is reduced generally. Inversely, it is increased with the fluctuation amplitude of the plate. In addition, different types of movement such as

moving forward, backward, hovering, etc. of the black ghost knife fish were also investigated by Youngerman et al. [14]. Their results have shown that different locomotion behaviors are dictated by different patterns of anal fin motion, these conclusions are very meaningful in the design of biomimetic fin in the future. In 2008, Shirgaonkar et al. [15] also found that the propulsive force increases with frequency, amplitude, and wavelength. Applying the above results and some other influences such as phase difference and structural characteristics, Ajith et al. [16] optimized the design for median paired fin (MPF) to create a better performance without extending the fin.

In underwater biomimetic robot design, it is necessary to calculate the efficiency of engine thrust, auxiliary thrust, drag force, and determine that how to generate more thrust and reduce drag force. These have been not studied well. The previous research has concentrated on optimizing the propulsion efficiency on the undulating fin, therefore, in the present study, CFD analyses have been carried out investigating the drag force as a function of several wavelengths. Once calculating the drag force, the essential power of the propulsion motor can easily be chosen for the operating robot. For those purposes, ANSYS Fluent Software [17] was applied to compute Navier-Stokes equation, energy equation, and hydrodynamic force numerically. The number of wavelengths was varied from one to three to see the change in drag force.

## 2 Methodology

### 2.1 Physical model

For the convenience of calculation, a 2D geometry can be applied. In this case, it initially has a sine-wave profile with wavelength  $\lambda$  and amplitude  $A$  as shown in Fig. 2. The full length is  $L$ . A domain of length  $H$  and height  $W$  was chosen for fluid around the fin. In the real world, the fin is moving forward with velocity  $u$ . However, in this study, the fin would remain stationary and everything else will move relative to it. The water would come in through the inlet with its magnitude  $u$  and leave the domain through the outlet was given as pressure outlet with relative pressure  $p$ . The top and bottom edges of the water channel were set as a stationary wall with specified shear. In this study, the fin oscillates about the  $z$ -axis with a frequency  $f$ . The parameters values of Curet's experiment can be used for this problem to compare the results. The model was built in SpaceClaim, all parameters are shown in Table 1.

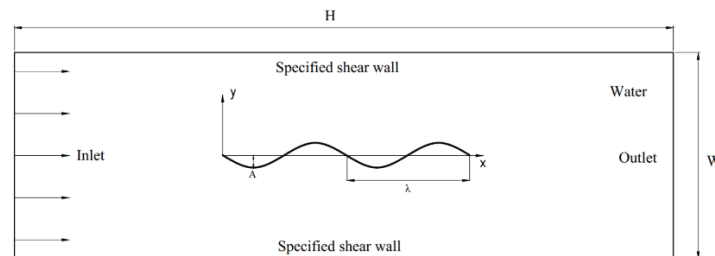


**Fig. 1.** 2D model of the undulating fin.

All points of the fin oscillate with the same frequency  $f$  and amplitude  $A$  but different phases from each other. Specifically, two points separated by a distance  $x$  are out of phase by an angle  $\theta$ . So the motion of the fin at a time  $t$  can be defined by:

$$y(x, t) = A \sin(2\pi ft - \theta) \quad (1)$$

$$\theta = \frac{2\pi x}{\lambda} \quad (2)$$

**Table 1.** Parameters used for computation

Parameter	Value
H (mm)	800
W (mm)	250
L (mm)	300
$e$ (mm)	0.5
$\lambda$ (cm)	15
$A$ (cm)	2
$p$ (Pa)	0
$f$ (Hz)	4

To examine the behavior of flow for moving objects in the fluid domain, the Navier-Stokes equation and some relevant equations are used. The Navier–Stokes equations are mathematically expressed conservation of momentum and conservation of mass for Newtonian fluids. It has become the most basic equation, the premise for the development of the fluid mechanics' field. Today, it is widely used in many phenomena of scientific and different engineering disciplines.

It can be used to simulate the flow around subsonic and supersonic flying vehicles [18]; the flow outside the racing car [19]; the water flow in a pipe [20], etc. In incompressible flow, it can be written as:

$$\rho \frac{dU}{dt} = -\nabla p + \mu \nabla^2 U + F \quad (3)$$

$$\nabla \cdot U = 0 \quad (4)$$

where  $\rho$  is the density of the fluid;  $\mu$  is the dynamic viscosity of the fluid;  $U = (u, v, w)$  is the fluid velocity vector;  $F$  is the external force acting on the fluid (gravity);  $p$  is the pressure;  $t$  is the time and  $\nabla$  is the Nabla operator, defined as

$$\vec{\nabla} = \vec{i} \frac{\partial}{\partial x} + \vec{j} \frac{\partial}{\partial y} + \vec{k} \frac{\partial}{\partial z} \quad (5)$$

In addition,  $k$ - $\varepsilon$  model was used to predict accurately the hydrodynamic drag of the fin and the turbulence that occurred in the model. Turbulence model  $k$ - $\varepsilon$  is the most popular model used in the computational fluid dynamics (CFD) approach to simulate the flow features for given physical conditions. In 2020, Takeshi et al. [21] applied  $k$ - $\varepsilon$  model to predict flow fields in urban areas. In another study, Gil Ho Yoon et al. [22] did not use this model to predict the flow field, instead, he used it for developing a new topology optimization by reducing the turbulent kinetic or the turbulent dissipation energies.  $k$ - $\varepsilon$  model gives a comprehensive description of turbulence by two transport equations. The first variable is the turbulent kinetic energy ( $k$ ), another is the rate of dissipation of turbulent kinetic energy ( $\varepsilon$ )

$$\frac{\partial(\rho k)}{\partial t} + \frac{\partial(\rho k U_j)}{\partial x_j} = \frac{\partial}{\partial x_j} \left[ \left( \mu + \frac{\mu_t}{\sigma_k} \right) \frac{\partial k}{\partial x_j} \right] + P_k + P_b - \rho \varepsilon - Y_M + S_k \quad (6)$$

$$\frac{\partial(\rho \varepsilon)}{\partial t} + \frac{\partial(\rho \varepsilon U_j)}{\partial x_j} = \frac{\partial}{\partial x_j} \left[ \left( \mu + \frac{\mu_t}{\sigma_\varepsilon} \right) \frac{\partial \varepsilon}{\partial x_j} \right] + C_{1\varepsilon} \frac{\varepsilon}{k} (P_k + C_{3\varepsilon} P_b) - C_{2\varepsilon} \rho \frac{\varepsilon^2}{k} + S_\varepsilon \quad (7)$$

where  $k$  is the turbulent kinetic energy;  $\varepsilon$  is the dissipation of KE;  $\mu_t$  is the turbulent viscosity;  $g$  is the gravity acceleration;  $P_k$  is the turbulence production;  $P_b$  is the affection of buoyancy;  $Y_M$  is the contribution of pulsatile expansion incompressible turbulence;  $S_k$  and  $S_\varepsilon$  are user-defined source terms

Some relevant constants in the standard  $k$ - $\varepsilon$  model are  $C_{1\varepsilon} = 1.44$ ;  $C_{2\varepsilon} = 1.92$ ;  $C_{3\varepsilon} = 0.09$ ;  $\sigma_k = 1$ ;  $\sigma_\varepsilon = 1.3$ . The remaining constants are determined by:

$$\mu_t = \rho C_\mu \frac{k^2}{\varepsilon} \quad (8)$$

$$P_k = \mu_t S^2 \quad (9)$$

$$P_b = \beta g_i \frac{\mu_t}{Pr_t} \frac{\partial T}{\partial x_i} \quad (10)$$

where  $Pr_t$  is the turbulent Prandtl number for energy. In the standard model,  $Pr_t = 0.85$ ;  $g_i$  is the gravitational vector component in  $i^{\text{th}}$  direction;  $\beta$  is the thermal expansion coefficient,  $\beta = 0$  in the present study because the water is isothermal. In general, it is defined as:

$$\beta = -\frac{1}{\rho} \left( \frac{\partial \rho}{\partial T} \right)_p \quad (11)$$

The hydrodynamic force acting on the object is written by:

$$F_D = \frac{1}{2} \rho C_D A v^2 \quad (12)$$

where  $\rho$  is the fluid density;  $A$  is the reference area of fin;  $v$  is the stream velocity;  $C_D$  is drag coefficient, depending on the shape of the object.

The parameters of fluid domain are the water at temperature  $T = 25^\circ\text{C}$ , density  $\rho = 998.2 \text{ kg/m}^3$ , dynamic viscosity  $\mu = 1.003 \text{ mPa.s}$

## 2.2 Numerical methods

In general, the simulation model has three regions that are necessary to mesh such as the enclosure, the body of influence (BOI), and the boundary layer. All these regions are generated with tetrahedral mesh since they make the simulation easy to achieve convergence. The enclosure is the volume analyzed to study how water interacts with the fin and what forces are generated, this region has a larger grid size than other regions to save computing resources as well as computation time. In the BOI, the mesh must be generated densely with a smaller size because it is important to have accurate results in the vicinity of the fin. Finally, the mesh near the wall region needs to be meshed to capture the effect of the boundary layer that forms along the walls, so edge sizing and inflation method are used to fulfill this requirement to accurately capture the flow physics here. The complete meshed model is shown in Fig. 2.

To simulate the special movement of the fin and the deformation of mesh during the analysis process, a user defined function (UDF) written by C programming language and Dynamic Mesh method is used. Specifically, smoothing, layering and refining are used with minimum and maximum length scales are 0.001m and 0.008m. The pressure-velocity coupling is realized with the COUPLED algorithm. The gradient is discretized with the least squares cell based (LSCB) while Navier-Stokes momentum, turbulent kinetic energy, and turbulent dissipation rate are discretized with the second-order upwind because of its easy convergence. To avoid the negative volume, the fin is simulated with a small step size of 0.005s in 1000 time steps. All of them are conducted in ANSYS Fluent software.

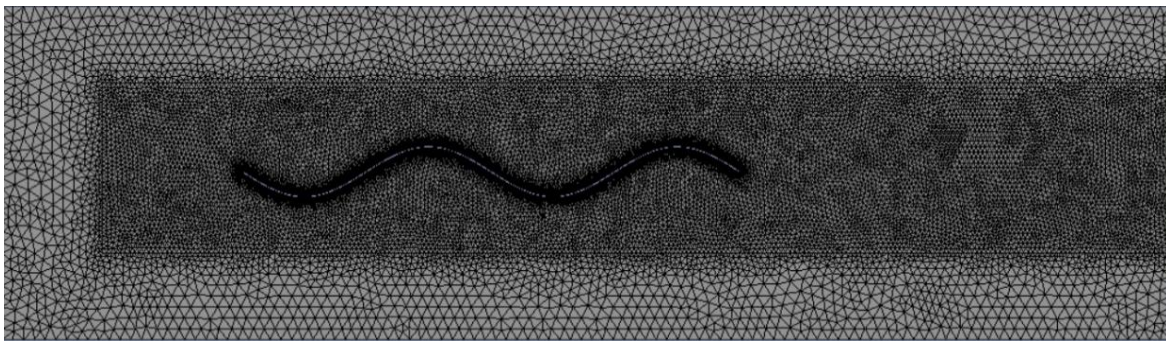


Fig. 2. The dense triangle mesh around the fin

## 3 Results and Discussion

For a more intuitive approach to Curret's experimental results, some CFD analyses were carried out. The fluid domain around the fin is water at temperature  $T = 25^{\circ}C$ ,  $\rho = 998.2 \text{ kg/m}^3$ , dynamic viscosity  $\mu = 0.001003 \text{ kg/ms}$ .

Fig. 3 depicts the velocity contour captured at  $t = 2.5\text{s}$  in the case that the fin oscillates periodically with the frequency  $f$ , the inlet velocity  $u = 0.18 \text{ m/s}$  and the number of wave  $N = 2$ . Different colors represent different velocities around the domain. Flow velocity has a small value in regions that are far from the influence of fin, behind the fin is where the flow velocity is highest. This indicates that the water particles move backward during the movement of the fins due to the fin's special oscillation. All points along the fin oscillate with the same frequency but different phases from each other, this produces a wave transmit along the body length with velocity  $v = \lambda.f$ . The higher the frequency, the higher velocity of the wave. In the end, this wave continues to transfer motion to the water particles behind, causing the water particles to move in the direction of wave propagation. According to the law of forces and reactions, the water also impacts an opposite force on the fin, causing it to accelerate. This plays an important role in future research about propulsion improvement. The experimental results also measured that repulsion and found that repulsion also increases with frequency [4].

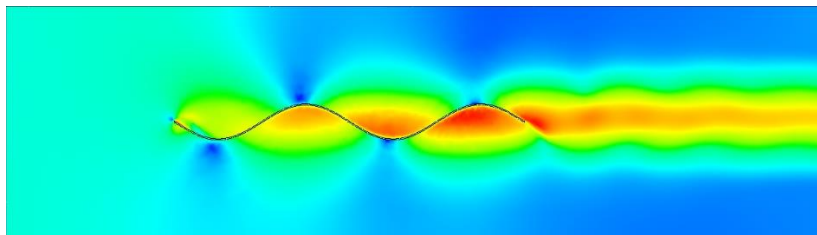
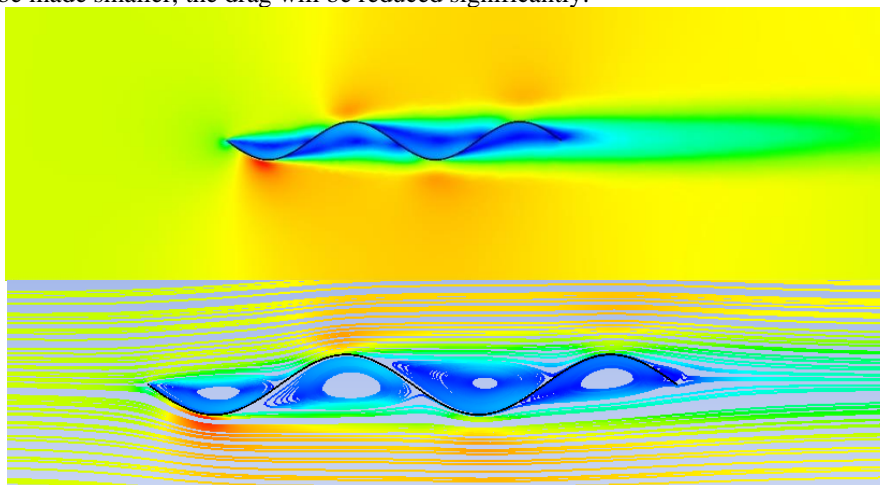


Fig. 3. The velocity fields surrounding the bionic undulating fin with the inlet velocity  $u = 0 \text{ m/s}$ , the number of waves  $N = 2$ , the frequency  $f = 4 \text{ Hz}$

The hydrodynamic analysis was conducted to measure the drag force and drag coefficient as a function of waves  $N$  at  $N = 1, 2, \text{ and } 3$ ; frequency  $f = 0$ ; velocity inlet  $u = 0.18 \text{ m/s}$ . Fig. 4 represents the velocity contour and streamlines when the

fin was held stationary ( $f = 0$ ), the fin has two waves and the flow velocity was constant at 0.18 m/s. The drag is generated due to the pressure difference in front and behind the model. The water velocity has the highest value at the first surface in contact with the flow since the sine-wave profile of the fin created adverse contact angles along the stream, flow separation occurred at this surface and causes the flow to change direction suddenly. It is easy to see that some wake regions are created along the fin. In this wake region, a considerable pressure misplacement occurs and creates a low-pressure area. In regions with higher pressure, water will be sucked into these regions and produce vortices. This low-pressure area also has the same effect as a vacuum causing drag on the model. From the above statements, if this low-pressure area can be made smaller, the drag will be reduced significantly.



**Fig. 4.** Velocity contours, streamlines surrounding the bionic undulating fin with the inlet velocity  $u = 0.18$  m/s, number of waves  $N = 2$ , the frequency  $f = 0$

Fig. 5 surveys the drag force acting on the model within five seconds. From the graph, it can be seen that for a very short period in the early stage, the resistance force has a quite large value because of the sudden separation when the flow makes contact with the fins, this leads to the development of a large low-pressure region and causes a lot of resistance. Then, the flow has become stable, the wake region becomes narrowed and the drag force is now reduced to a small constant value ( $\sim 0.01$  N).

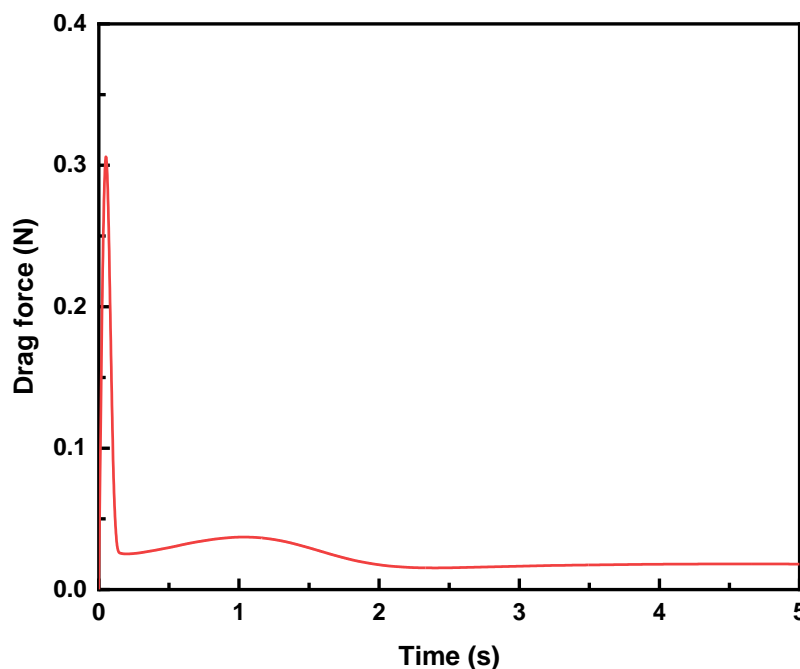


**Fig. 5.** Drag force acting on the undulating fin at  $u = 0.18$  m/s,  $N = 2$

Figs. 6 and 7 show the contours of the velocity distribution in the case of one and three wavelengths. In general, the velocity distribution in these two cases is quite similar to the first case ( $N = 2$ ). However, there is a significant difference in the size of the wake regions. As mentioned in the first case, the wake region affects the resistance of most hydrodynamic models in general and bionic fin in particular. In the case of  $N = 3$ , there are six vortices are generated. Moreover, the wake at the back of the model is larger and based on the color distribution, it can be identified that the water velocity here

is lower than in the first case. In the case of  $N = 1$ , on the contrary, the number of vortices is significantly reduced and the wake is very small. It can be said that changing the fin profile affects the area of the generated low-pressure region.

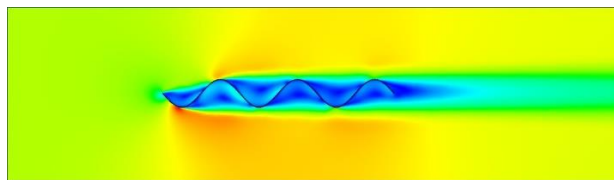


**Fig. 6.** Velocity contour surrounding the bionic undulating fin with the inlet velocity  $u = 0.18$  m/s, number of waves  $N = 3$ , the frequency  $f = 0$

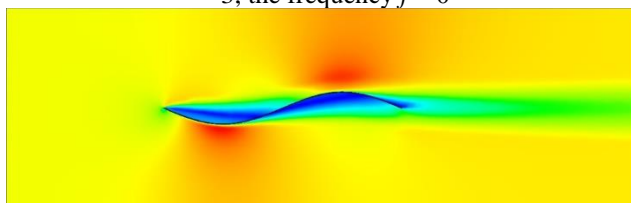


**Fig. 7.** Velocity contour surrounding the bionic undulating fin with the inlet velocity  $u = 0.18$  m/s, number of waves  $N = 1$ , the frequency  $f = 0$

Fig. 8 compares drag force acting on the fin in the first five seconds between three cases ( $N = 1, 2$ , and  $3$ ). The drag force in these cases shows the same trends, large at first and stable later. The difference in resistance force magnitude is not much, but it can be seen that it is larger as the number of waves increases. This can be explained by the fact that when the fin length and the amplitude are kept constant, but increasing the number of wavelengths, the contact angle between the flow and the body increases, this leads to a development in the wake region as mentioned above. Therefore, the drag force tends to increase. Fig. 9 demonstrates the drag coefficient at three different speeds of the fin. As can be seen from the numerical results, the drag coefficient increases almost linearly with the fin's speed. Table 2 shows the specific values of drag force and drag coefficient received from ANSYS Fluent Solver at  $u = 0.1$  m/s;  $0.18$  m/s and  $0.26$  m/s, respectively. The obtained numerical results are approximate with the experiments of Curet, showing the reasonableness of the proposed numerical methods.

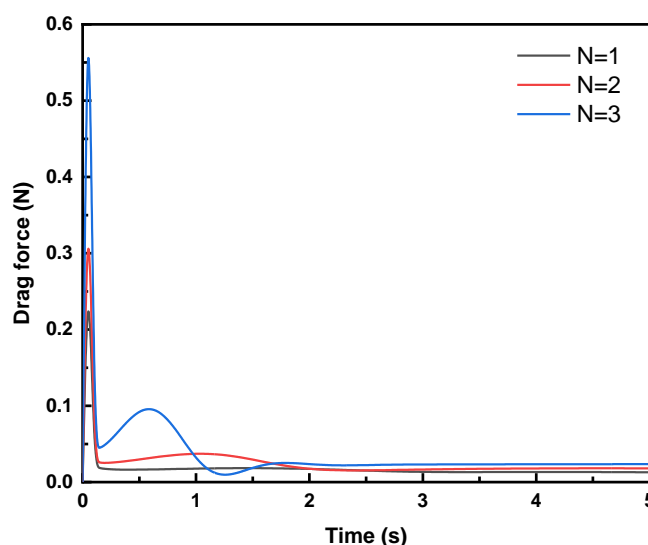


**Fig. 8.** Drag force acting on the undulating fin with  $u = 0.18$  m/s at different number of wavelengths

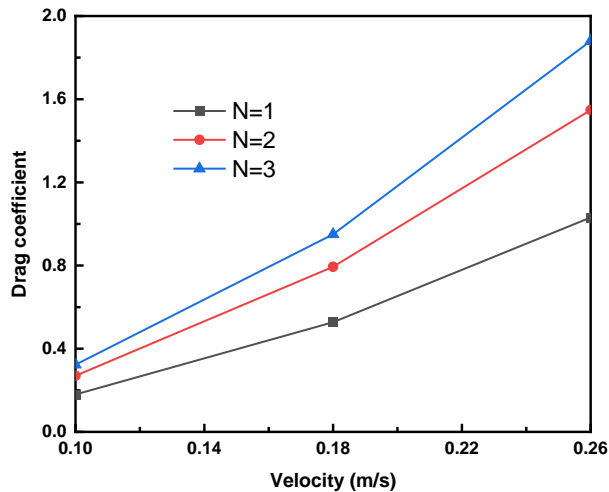


**Fig. 9.** The drag coefficients for undulatory fin at the different velocities

**Table 2.** Numerical results from ANSYS CFD-Post at different velocities of the fin

Velocity (m/s)	Drag Force (N)	Drag Coefficient (N)
0.1	0.013	0.27
0.18	0.017	0.79
0.26	0.019	1.55

#### 4 Conclusions

In this paper, SpaceClaim was used to design the profile of the bionic fin veil. Then the model was meshed with the adapted method and analyzed to understand the interaction and behavior of the water around it. For finding out what causes repulsion, a user defined function (UDF) was immersed to simulate the oscillation of the profile accurately. Velocity field contours showed that the periodic motion of the model generates thrust, which is in agreement with previous experiments. Furthermore, by keeping the fin in a stationary state, the influence of the number of wavelengths on the drag force is shown clearly. The drag force and average drag coefficient are predicted to increase when the number of waves gets larger. By using CFD approach, the results have become the basis to help in designing and optimizing the working performance of the robot. In addition, it helps to reduce the time and cost of testing in future related designs.

#### Acknowledgement

We acknowledge the support of time and facilities from Ho Chi Minh City University of Technology (HCMUT), VNU-HCM for this research.

#### References

- [1] G. Shi, Q. Xiao, Numerical investigation of a bio-inspired underwater robot with skeleton-reinforced undulating fins, *Fluids* 87 (2021) 75-91.
- [2] H. Zhou, T. Hu, H. Xie, D. Zhang, L. Shen, Computational Hydrodynamics and Statistical Modeling on Biologically Inspired Undulating Robotic Fins: A Two-Dimensional Study, *Bionic Engineering* 7 (2010) 66-76.
- [3] Y. Zhang, J. He, K.H. Low, Parametric Study of an Underwater Finned Propulsor Inspired by Bluespotted Ray, *Bionic Engineering* 9 (2012), 166-176.
- [4] O.M. Curet, N.A. Patankar, G.V. Lauder, M.A. MacIver, Mechanical properties of a bio-inspired robotic knifefish with an undulatory propulsor, *Bioinspiration & Biomimetics* 6 (2011) 026004
- [5] H. Zhou, T. Hu, K.H. Low, L. Shen, Z. Ma, G. Wang, H. Xu, Bio-inspired Flow Sensing and Prediction for Fish-like Undulating Locomotion: A CFD-aided Approach, *Bionic Engineering* 12 (2015) 406-417
- [6] T.L. Le, J.C. Chen, B.C. Shen, F.S. Hwu and H.B. Nguyen, Numerical investigation of the thermocapillary actuation behavior of a droplet in a microchannel, *Int. J. Heat Mass Transfer* 83 (2015) 721-730.
- [7] T.L. Le, J.C. Chen, F.S. Hwu and H.B. Nguyen, Numerical study of the migration of a silicone plug inside a capillary tube subjected to an unsteady wall temperature gradient, *Int. J. Heat Mass Transfer* 97 (2016) 439-449.
- [8] T.L. Le, J.C. Chen, and H.B. Nguyen, Numerical study of the thermocapillary droplet migration in a microchannel under a blocking effect from the heated wall, *Appl. Thermal Eng.* 122 (2017) 820-830.
- [9] T.L. Le, J.C. Chen, and H.B. Nguyen, Numerical investigation of the forward and backward thermocapillary motion of a water droplet in a microchannel by two periodically activated heat sources, *Numerical Heat Transfer, Part A: Applications* 79(2) (2020) 146-162.

- [10] T.L. Le, N.T. Tien, A CFD study on hydraulic and disinfection efficiencies of the body sterilization chamber, *Annals of the Romanian Society for Cell Biology* 25(2) (2021) 3998-4004.
- [11] T.L. Le, T.D. Hong, Computational fluid dynamics study of the hydrodynamic characteristics of a torpedo-shaped underwater glider, *Fluids* 6 (2021) 252.
- [12] I.D. Neveln, R. Bale, A.P.S Bhalla, O.M. Curet, N.A. Patankar, M.A. MacIver, Undulating fins produce off-axis thrust and flow structures, *Experimental Biology* 217 (2014) 201-213.
- [13] Y.H. Zhang, J.H. He, K.H. Low, Numeric Simulation on the Performance of an Undulating Fin in the Wake of a Periodic Oscillating Plate, *Advanced Robotic Systems* (2013) 56439.
- [14] D.Y. Eric, E.F. Brooke, V.L. George, Locomotion of free-swimming ghost knifefish: anal fin kinematics during four behaviors, *Zoology* (2014) 25401.
- [15] A.A. Shirgaonkar, O.M. Curet, N.A. Patankar, M.A. MacIver, The hydrodynamics of ribbon-fin propulsion during impulsive motion, *Experimental Biology* 211 (2008) 3490-3503.
- [16] A.A. Meera, A.P. Sudheer, Design Optimization of the Biomimetic Undulating Fin of a Knife Fish Robot, *Automation, Mobile Robotics & Intelligent Systems* (2016) 14313.
- [17] ANSYS Fluent User's Guide.
- [18] A. Viviani, A. Arovitola, G. Pezzella, C. Rainone, CFD design capabilities for next generation high-speed aircraft, *Acta Astronautica* 178 (2021) 143–158.
- [19] K. Kurec, M. Remer, J. Piechna, The influence of different aerodynamic setups on enhancing a sports car's braking, *International Journal of Mechanical Sciences* 164 (2019) 105140.
- [20] M. Prasada, V. Gopikaa, A. Sridharanb, S. Paridab, Pipe wall thickness prediction with CFD based mass transfer coefficient and degradation feedback for flow accelerated corrosion, *Progress in Nuclear Energy* 107 (2018) 205–214.
- [21] T. Ishihara, G.W. Qian, Y.H. Qi, Numerical study of turbulent flow fields in urban areas using modified k- $\epsilon$  model and large eddy simulation, *Wind Engineering & Industrial Aerodynamics* 206 (2020) 104333.
- [22] G.H. Yoon, Topology optimization method with finite elements based on the k- $\epsilon$  turbulence model, *Comput. Methods Appl. Mech. Engrg.* 361 (2020) 112784.